International Journal of Modern Physics A
Vol. 34, No. 11 (2019) 1950062 (16 pages)

DOI: 10.1142/S0217751X19500623

Bounds on dipole moments of tau-neutrino from single photon searches in $SU(4)_L \times U(1)_X$ model at CLIC and ILC energies

D. T. Binh*

Institute of Theoretical and Applied Research,
Duy Tan University, Hanoi 10000, Vietnam
dtbinh@iop.vast.ac.vn

Vo Van On

Department of Physics, Faculty of Natural Sciences,
University of Thu Dau Mot, Binh Duong, Vietnam
Group of Computational Physics, Faculty of Natural Sciences,
University of Thu Dau Mot, Binh Duong, Vietnam
onvv@tdmu.edu.vn

H. N. Long

Institute of Physics, Vietnam Academy of Science and Technology,
10 Dao Tan, Ba Dinh, Hanoi, Vietnam
hnlong@iop.vast.ac.vn

Received 9 March 2018
Revised 15 August 2018
Accepted 7 September 2018
Published 10 May 2019

We investigate the dipole moments of the tau-neutrino at high-energy and high luminosity at linear electron–positron colliders, such as CLIC or ILC through the analysis of the reaction $e^+e^- \to \nu\bar{\nu}\gamma$ in the framework of the $SU(4)_L \times U(1)_X$ model. The limits on dipole moment were obtained for integrated luminosity of $\mathcal{L} = 250$–$1000\ \mathrm{fb}^{-1}$ and mass ranging from 0.25 to 1.0 TeV. The estimated limits for the tau-neutrino magnetic and electric dipole moments at 95% of confidence level are $\mu_{\nu_\tau} \leq 4.83 \times 10^{-9}$ and $d_{\nu_\tau} \leq 2.04 \times 10^{-19}$ improved by 2–3 orders of magnitude compared to L3 and complement previous studies on the dipole moments.

Keywords: Nonstandard model neutrinos; electric and magnetic moments; neutral currents; models beyond the standard model.

PACS numbers: 14.60.St, 13.40.Em, 12.15.Mm, 12.60.−i

*Corresponding author.

Table 1. Experimental limits on the magnetic moment of the tau-neutrino.

Experiment	Method	Limit	C.L.	Reference
Borexino	Solar neutrino	$\mu_{\nu_\tau} < 1.9 \times 10^{-10}\mu_B$	90%	15
E872 (DONUT)	Accelerator $\nu_\tau e^-$, $\bar{\nu}_\tau e^-$	$\mu_{\nu_\tau} < 3.9 \times 10^{-7}\mu_B$	90%	16
CERN-WA-066	Accelerator	$\mu_{\nu_\tau} < 5.4 \times 10^{-7}\mu_B$	90%	17
L3	Accelerator	$\mu_{\nu_\tau} < 3.3 \times 10^{-6}\mu_B$	90%	28

1. Introduction

Experiments and theoretical studies of solar neutrino oscillation[1] and atmospheric neutrino oscillation[2] gave strong evidence of the nonzero mass of neutrino. A massive neutrino can have nontrivial electromagnetic properties through radiative correction and the coupling between neutrinos and photon is possible. The most important electromagnetic processes of the direct neutrino couplings with photon are

- The radiative decay of a heavy neutrino into a lighter neutrino with emission of a photon $\nu \to \nu + \gamma$.[3,4]
- Photon decays into neutrino–antineutrino pair in plasma: $\gamma \to \nu\bar{\nu}$.[5]

Neutrino one-photon interactions are of interest since they may play a key role in elucidating the solar neutrino puzzle, which can be explained by a large neutrino magnetic moment[6] or a resonant spin flip induced by Majorana neutrinos.[7,8]

A Dirac neutrino, with Standard Model (SM)[9–11] interactions, has a magnetic moment given by[12]

$$\mu_{\nu_i} = \frac{3m_e G_F}{4\sqrt{2}\pi^2} m_{\nu_i} \approx 3 \times 10^{-19} \left(\frac{m_{\nu_i}}{\text{eV}}\right) \mu_B \,, \tag{1}$$

where $\mu_B = \frac{e}{2m_e}$ is the Bohr magneton. Current limits on these magnetic moments are several orders of magnitude larger,[13–18] therefore a magnetic moment close to these limits would indicate a window for probing effects induced by new physics beyond the SM.[24] Similarly, a neutrino electric dipole moment (EDM) will also imply new physics and they will be of relevance in astrophysics and cosmology, as well as terrestrial neutrino experiments.[25]

The current best limit on μ_{ν_τ} has been obtained in the Borexino experiment which explores solar neutrinos.[15] Some experimental limits on the magnetic moment of the tau-neutrino are shown in Table 1. On the other hand, the current limit on EDM of tau-neutrino (d_{ν_τ}) is[26,27]

$$d_{\nu_\tau} < 5.2 \times 10^{-17} \text{ e} \cdot \text{cm} \,. \tag{2}$$

Single photon events in e^-e^+ annihilation at the Z boson resonance is sensitive to new physics.[21–23] The photon signals come from main sources such as (a) initial radiation with neutrino pair or $f\bar{f}$ pair, (b) QED event, e.g. $e^+e^- \to f\bar{f}\gamma$ and (c) possible new physics signatures.

The process $e^-e^+ \to \gamma +$ "missing energy" is an efficient way to explore new physics. In the SM, the missing energy can be carried by neutrino which comes from the Z exchange in the s-channel and from the t-channel through W exchange. Beyond SM, the "missing energy" could come from new generation of neutrinos, radiative production of new weakly interacting particle or new particles decay into photon.

Near the Z boson resonance, photon comes from the initial state radiation has energy less than a few GeV and tends to be emitted along the beam. Single photon events come from radiative production are expected to be the result of new physics scenarios and carry a significant fraction of the beam energy and the polar angle distribution of these photons are not as forward and backward peaked as that of photons come from initial radiation state.

The L3 collaboration[28,29] searches for new physics by manifesting the direct coupling between the Z and photon or a direct radiative transition in the final state, by using detector-simulated $e^+e^- \to \bar{\nu}\nu\gamma$ events, random trigger events, and large angle $e^+e^- \to e^+e^-$ events to evaluate the selection efficiency. To select events, the energy cluster must be greater than 15 GeV and its polar angle must be in the range $20^\circ < \theta < 34.5^\circ$, $44.5^\circ < \theta < 135.5^\circ$ or $145.5^\circ < \theta < 160^\circ$.

In the SM, the bounds on μ_{ν_τ} and d_{ν_τ} have been obtained in Refs. 30 and 31 through the analysis of the process $e^+e^- \to \bar{\nu}\nu\gamma$ near the Z boson-resonance, and the latter give main contribution to the bound of the μ_{ν_τ} and d_{ν_τ}. Therefore, the existence of new neutral gauge boson Z' would give stronger bounds on μ_{ν_τ} and d_{ν_τ} as one would expect. Hence, it is natural to extend the work to find the bounds of μ_{ν_τ} and d_{ν_τ} in beyond the Standard Model (BSM).

Additional neutral gauge bosons appear in most BSM such as left–right symmetric models (LRSM),[32,33] models of composite gauge bosons[34] or the $SU(3)_C \times SU(3)_L \times U(1)_X$ (3-3-1) models.[35–44] The bounds of μ_{ν_τ} and d_{ν_τ} have been investigated in Refs. 45–55. However, it is possible to study some phenomenological features associated with this extra neutral gauge boson through models with gauge symmetry $SU(3)_C \times SU(4)_L \times U(1)_X$, also called 3-4-1 models.[38,56–58] In this model there exit two new neutral gauge bosons. Similarly to the Z boson, the main contribution to the dipole moment of the neutrino is through the Z' boson resonance in s-channel which would result in large constraint to the neutrino dipole moment in the above-mentioned model.

In the framework of the 3-4-1 model, the puzzle of the large magnetic moment of neutrino with its small mass was firstly considered in Ref. 59. The interaction of Z' boson with neutrino in this model allow the possibility of Z' decay into a pair of massive neutrino ($\Gamma_{Z' \to \bar{\nu}\nu}$). The creation of massive neutrino through Z' resonance at LHC is studied in Ref. 60.

Our aim in this paper is to get the bounds of the magnetic and electric dipole moments of the neutrino by analyzing the reaction $e^+e^- \to \nu\bar{\nu}\gamma$ in the framework of the $SU(4)_L \times U(1)_X$ model. We will focus on the anomalous magnetic moment (MM) and the electric dipole moment (EDM) of massive tau-neutrino.

The dominant contribution arises from the exchange of the Z, Z' bosons through s-channel.[30] The dependence on the magnetic moment (μ_{ν_τ}) and the electric dipole moment (d_{ν_τ}) comes from the radiation of the photon observed by the neutrino or antineutrino in the final state, while the main background of this reaction is initial photon radiation and a neutrino pair. We will set limits on the tau-neutrino MM and EDM according to the ratio of the $SU(4)\times U(1)_X$ scale versus $SU(2)_L\times U(1)_Y$ scale and for integrated luminosity of 250–1000 fb^{-1} with center-of-mass energy between 0.25 and 1.0 TeV which can be archived in the next generation of linear colliders, namely, the International Linear Collider (ILC)[62] and the Compact Linear Collider (CLIC).[63]

This paper is organized as follows. In Sec. 2, we will briefly review the 3-4-1 model. Then in Sec. 3, we present the calculation of the process $e^+e^- \to \nu\bar{\nu}\gamma$ in the context of a $SU(4)_L \times U(1)_X$ model. Finally, we present our results and conclusions in Sec. 4.

2. Minimal 3-4-1 with Right-Handed Neutrinos

The $SU(4)_L\times U(1)_X$ model was originally proposed in Refs. 38, 56, 57. The minimal $SU(4)_L \times U(1)_X$ model was systematically studied in Ref. 58. In this section we will briefly review the model. The leptonic structure of the $SU(4)_L \times U(1)_X$ model is arranged as

$$f_{aL} = (\nu_a, l_a, l_a^c, \nu_a^c)_L^T \sim (1,4,0)\,, \quad a = e,\mu,\tau\,,$$

where $\nu_L^c \equiv (\nu_R)^c$ and the charge conjugation of f_{aL}

$$f_{aR}^c \equiv (f_{aL})^c = \left(\nu_{aR}^c, l_{aR}^c, l_{aR}, \nu_{aR}\right)^T .$$

One quark generation is arranged into quadruplet

$$Q_{3L} = (u_3, d_3, T, T')_L^T \sim \left(3, 4, \frac{2}{3}\right),$$

$$u_{3R} \sim \left(3,1,\frac{2}{3}\right), \quad d_{3R} \sim \left(3,1,-\frac{1}{3}\right),$$

$$T_R \sim \left(3,1,\frac{5}{3}\right), \quad T'_R \sim \left(3,1,\frac{2}{3}\right).$$

The two other quark generations are arranged as antiquadruplet

$$Q_{\alpha L} = \left(d_\alpha, -u_\alpha, D_\alpha, D'_\alpha\right)_L^T \sim \left(3, 4^*, -\frac{1}{3}\right), \quad \alpha = 1,2\,,$$

$$u_{\alpha R} \sim \left(3,1,\frac{2}{3}\right), \qquad d_{\alpha R} \sim \left(3,1,-\frac{1}{3}\right),$$

$$D_{\alpha R} \sim \left(3,1,-\frac{4}{3}\right), \quad D'_{\alpha R} \sim \left(3,1,-\frac{1}{3}\right).$$

The Higgs sector consisting four Higgs quadruplets is given below

$$
\begin{aligned}
\chi &= \left(\chi_1^0, \chi_2^-, \chi_3^+, \chi_4^0\right)^T \sim (1,4,0)\,,\\
\Phi &= \left(\Phi_1^-, \Phi^{--}, \Phi^0, \Phi_2^-\right)^T \sim (1,4,-1)\,,\\
\rho &= \left(\rho_1^+, \rho^0, \rho^{++}, \rho_2^+\right)^T \sim (1,4,1)\,,\\
\eta &= \left(\eta_1^0, \eta_2^-, \eta_3^+, \eta_4^0\right)^T \sim (1,4,0)
\end{aligned}
\tag{3}
$$

and one symmetric decuplet ($\mathbf{10}_S$) as

$$
H \sim (1,\mathbf{10},0) = \frac{1}{\sqrt{2}}\begin{pmatrix} \sqrt{2}H_1^0 & H_1^- & H_2^+ & H_2^0 \\ H_1^- & \sqrt{2}H_1^{--} & H_3^0 & H_3^- \\ H_2^+ & H_3^0 & \sqrt{2}H_2^{++} & H_4^+ \\ H_2^0 & H_3^- & H_4^+ & \sqrt{2}H_4^0 \end{pmatrix}. \tag{4}
$$

The necessary vacuum expectation value (VEV) structure is given by

$$
\begin{aligned}
\langle\chi\rangle &= \left(0,0,0,\frac{V}{\sqrt{2}}\right)^T, \quad \langle\phi\rangle = \left(0,0,\frac{\omega}{\sqrt{2}},0\right)^T,\\
\langle\rho\rangle &= \left(0,\frac{v}{\sqrt{2}},0,0\right)^T, \quad \langle\eta\rangle = \left(\frac{u}{\sqrt{2}},0,0,0\right)^T
\end{aligned}
\tag{5}
$$

and

$$
\langle H\rangle = \frac{1}{2}\begin{pmatrix} 0 & 0 & 0 & \epsilon \\ 0 & 0 & v' & 0 \\ 0 & v' & 0 & 0 \\ \epsilon & 0 & 0 & 0 \end{pmatrix}. \tag{6}
$$

Then all fermions and gauge bosons get necessary masses.[58]

In the model, the gauge sector consists six charged/non-Hermitian gauge bosons and four neutral ones. The charged and non-Hermitian neutral gauge bosons defined through

$$
\begin{aligned}
P_\mu^{\mathrm{CC}} &= \frac{1}{2}\sum_a \lambda_a A_a\,, \quad a = 1,2,4,5,6,7,9,10,11,12,13,14\\
&= \frac{1}{\sqrt{2}}\begin{pmatrix} 0 & W'^+ & W_{13}^- & W_{14}^0 \\ W'^- & 0 & W_{23}^{--} & W_{24}^- \\ W_{13}^+ & W_{23}^{++} & 0 & W_{34}^+ \\ (W_{14}^0)^* & W_{24}^+ & W_{34}^- & 0 \end{pmatrix}_\mu = \frac{1}{\sqrt{2}}\begin{pmatrix} 0 & W'^+ & Y'^- & N^0 \\ W'^- & 0 & U^{--} & X'^- \\ Y'^+ & U^{++} & 0 & K'^+ \\ (N^0)^* & X'^+ & K'^- & 0 \end{pmatrix}_\mu .
\end{aligned}
\tag{7}
$$

The above gauge bosons mix each other, and the physical states are determined as[58]

$$W_\mu = \cos\theta W'_\mu - \sin\theta K'_\mu\,, \quad K_\mu = \sin\theta W'_\mu + \cos\theta K'_\mu\,, \tag{8}$$

where the mixing angle θ characterizing lepton number violation is given by

$$\tan 2\theta = \frac{4v'\epsilon}{V^2+\omega^2-u^2-v^2}\,. \tag{9}$$

For the $X-Y$ mixing, we obtain the physical states

$$Y_\mu = \cos\theta' Y'_\mu - \sin\theta' X'_\mu\,, \quad X_\mu = \sin\theta' Y'_\mu + \cos\theta' X'_\mu \tag{10}$$

with the mixing angle defined as

$$\tan 2\theta' = \frac{4v'\epsilon}{V^2-\omega^2-u^2+v^2}\,. \tag{11}$$

The masses of physical gauge bosons are determined as

$$\begin{aligned} m_W^2 &\simeq \frac{g^2}{4}\left(v^2+u^2+v''^2\right), \quad m_K^2 \simeq \frac{g^2}{4}(V^2+w^2+v''^2)\,, \\ m_X^2 &\simeq \frac{g^2}{4}(V^2+v^2+v''^2)\,, \quad m_Y^2 \simeq \frac{g^2}{4}(w^2+u^2+v''^2)\,. \end{aligned} \tag{12}$$

The four neutral gauge bosons are the photon and three neutral gauge bosons labeled by Z_i, $i=1,2,3$.

2.1. *Charged currents*

Taking into account of the mixing among singly charged gauge bosons, we can express the above expression as follows:

$$-\mathcal{L}^{\rm CC} = \frac{g}{\sqrt{2}}\Big(J_W^{\mu-}W_\mu^+ + J_K^{\mu-}K_\mu^+ + J_X^{\mu-}X_\mu^+ + J_Y^{\mu-}Y_\mu^+ + J_N^{\mu0*}N_\mu^0 + J_U^{\mu--}U_\mu^{++} + \text{H.c.}\Big)\,,$$

where

$$\begin{aligned} J_W^{\mu-} &= c_\theta\left(\bar\nu_{aL}\gamma^\mu l_{aL} + \overline{u_{3L}}\gamma^\mu d_{3L} - \bar u_{\alpha L}\gamma^\mu d_{\alpha L}\right) \\ &\quad - s_\theta\left(-\overline{\nu_{aR}}\gamma^\mu l_{aR} + \overline{T_L}\gamma^\mu T'_L + \overline{D'_{\alpha L}}\gamma^\mu D_{\alpha L}\right), \end{aligned} \tag{13}$$

$$\begin{aligned} J_K^{\mu-} &= c_\theta\left(-\overline{\nu_{aR}}\gamma^\mu l_{aR} + \overline{T_L}\gamma^\mu T'_L + \overline{D'_{\alpha L}}\gamma^\mu D_{\alpha L}\right) \\ &\quad + s_\theta\left(\bar\nu_{aL}\gamma^\mu l_{aL} + \overline{u_{3L}}\gamma^\mu d_{3L} - \bar u_{\alpha L}\gamma^\mu d_{\alpha L}\right), \\ J_X^{\mu-} &= c_{\theta'}\left(\overline{\nu^c_{aL}}\gamma^\mu l_{aL} + \overline{T'_L}\gamma^\mu d_{3L} - \overline{u_{\alpha L}}\gamma^\mu D'_{\alpha L}\right) \\ &\quad + s_{\theta'}\left(\overline{l^c_{aL}}\gamma^\mu \nu_{aL} + \overline{T_L}\gamma^\mu u_{3L} + \overline{d_{\alpha L}}\gamma^\mu D_{\alpha L}\right), \\ J_Y^{\mu-} &= c_{\theta'}\left(\overline{l^c_{aL}}\gamma^\mu \nu_{aL} + \overline{T_L}\gamma^\mu u_{3L} + \overline{d_{\alpha L}}\gamma^\mu D_{\alpha L}\right), \\ &\quad - s_{\theta'}\left(\overline{\nu^c_{aL}}\gamma^\mu l_{aL} + \overline{T'_L}\gamma^\mu d_{3L} - \overline{u_{\alpha L}}\gamma^\mu D'_{\alpha L}\right), \\ J_U^{\mu--} &= \overline{l^c_{aL}}\gamma^\mu l_{aL} + \overline{T_L}\gamma^\mu d_{3L} - \overline{u_{\alpha L}}\gamma^\mu D_{\alpha L}\,, \\ J_N^{\mu0*} &= \overline{\nu_{aL}}\gamma^\mu \nu^c_{aL} + \overline{u_{3L}}\gamma^\mu T'_L + \overline{D'_{\alpha L}}\gamma^\mu d_{\alpha L}\,. \end{aligned} \tag{14}$$

For precision, in the quark sector the CKM matrix will be appeared. In terms of mass eigenstates, the current in (13) has a new form

$$J_W^{\mu-} = c_\theta\Big(\bar{\nu}_{iL}\gamma^\mu V_{\rm PMNS}^{ij} l_{jL} + s_\theta\,\overline{\nu_{iR}}\gamma^\mu V_{\rm PMNS}^{ij} l_{jR}\Big) + \cdots\,. \tag{15}$$

2.2. *Neutral current*

The Lagrangian of the fermion is

$$L = i\sum_f \bar{f}\gamma^\mu D_\mu f + \text{H.c.}$$

The Lagrangian for neutral current extracted from above Lagrangian is determined as

$$L^{\rm NC} = g\bar{f}\gamma^\mu P_\mu^{\rm NC} f\,,$$

where $P_\mu^{\rm NC}$ is given in Ref. 58. Explicitly, the neutral current including the electromagnetic current is

$$-L^{\rm NC} = eJ_{\rm em}^\mu A_\mu + \frac{g}{2c_w}\sum_{i=1}^{3} Z_\mu^i \sum_f \bar{f}\gamma^\mu\big[g_V^i(f) - g_A^i(f)\gamma_5\big]f\,,$$

where

$$e = g\sin\theta_W\,,\quad t = \frac{g'}{g} = \frac{2\sqrt{2}\sin\theta_W}{\sqrt{1-4\sin^2\theta_W}}\,.$$

Here, $Z^{1,2,3}$ can be identified as $Z^1 \approx Z$, and $Z^{2,3} \approx Z'_{3,4}$ are exact eigenstates.

From explicit calculation, the needed couplings are given by

$$g_V^1(e) = \frac{c_W(-3c_{32}s_W - \sqrt{3}c_W)}{2\sqrt{3}}\,,\quad g_A^1(e) = \frac{c_W(c_{32}s_W - \sqrt{3}c_W)}{2\sqrt{3}}\,,$$

$$g_V^1(\nu) = c_W\left(\frac{1}{2}c_W - \frac{c_{32}s_W}{2\sqrt{3}}\right),\quad g_A^1(\nu) = c_W\left(\frac{1}{2}c_W - \frac{c_{32}s_W}{2\sqrt{3}}\right),$$

$$g_V^2(e) = -\frac{c_W c_\alpha c_{32}}{2\sqrt{3}}\,,\quad g_A^2(e) = \frac{c_W(c_\alpha c_{32} + \sqrt{2}s_\alpha)}{2\sqrt{3}}\,,$$

$$g_V^2(\nu) = -\frac{c_W\big(c_\alpha s_{32} - 2s_\alpha\big)}{2\sqrt{3}}\,,\quad g_A^2(\nu) = \frac{c_W\big(c_\alpha s_{32} + \sqrt{2}s_\alpha\big)}{2\sqrt{3}}\,,$$

$$g_V^3(e) = -\sqrt{3}c_W s_\alpha s_{32}\,,\quad g_A^3(e) = \frac{c_W(c_\alpha + s_\alpha s_{32})}{2\sqrt{3}}\,,$$

$$g_V^3(\nu) = \frac{c_W\big(2\sqrt{2}c_\alpha - s_\alpha s_{32}\big)}{2\sqrt{3}}\,,\quad g_A^3(\nu) = \frac{c_W\big(\sqrt{2}c_\alpha + s_\alpha s_{32}\big)}{2\sqrt{3}}\,,$$

where $s_W \equiv \sin\theta_W$, $c_W \equiv \cos\theta_W$ and

$$s_{32} = \frac{2\sqrt{2}}{\sqrt{8+3t^2}}\,,\quad c_{32} = \frac{-\sqrt{3}t}{\sqrt{8+3t^2}}\,,\quad t_{2\alpha} = \frac{2\sqrt{8+3t^2}w^2}{9V^2-(7+3t^2)w^2}\,.$$

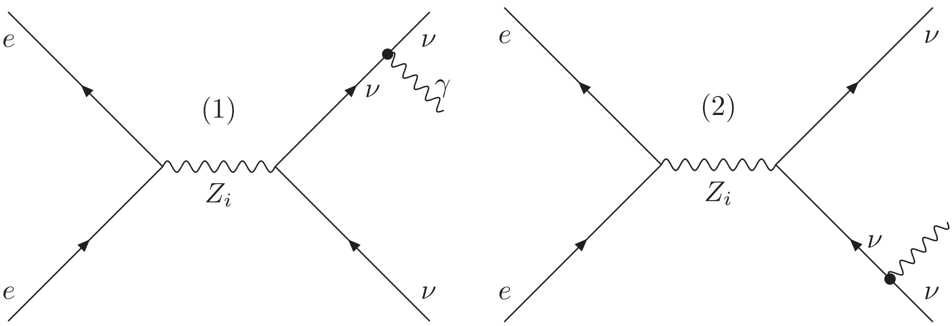

Fig. 1. Feynman diagrams contributing to process $e^+e^- \to \bar{\nu}\nu\gamma$ in the $SU(4)_L \times U(1)_X$ model.

3. The Total Cross-Section

The main background of the process $e^+e^- \to \bar{\nu}\nu\gamma$ is from the initial gamma radiation with a neutrino pair and photon from initial and final state radiation with a lepton pair in which the lepton pair escape the detection ($e^+e^- \to l^+l^-\gamma$, $l = e, \mu, \tau$). However, the energy of this type of photon is small at order of several GeVs and the angle distribution is along the beam (forward and backward peaked). Therefore, in the following if we apply the phase space cut requirement for the energy and the angle distribution, then the contribution of the background to the cross-section is negligible.

The Feynman diagrams giving the most important contribution to the cross-section of the process $e^+e^- \to \bar{\nu}_\tau\nu_\tau\gamma$ are shown in Fig. 1. Since the W and photon exchange diagrams amounting to just 1% corrections in the relevant kinematic regime hence will be neglected.[64,65] The main contribution comes from the s channel through neutral gauge boson Z_i.

We have assumed the normal hierarchy of neutrino mass[66] and since the cross-section is proportional to the square of the lepton dipole moment meaning the square of the lepton mass. Therefore the contribution of ν_e, ν_μ is a small fraction compare to ν_τ. Besides that, the current best limit for μ_{ν_τ} is from Borexino experiment[15]

$$\mu_{\nu_\tau} < 1.9 \times 10^{-10}\mu_B\,.$$

The current best bound for ν_e is[19]

$$\mu_{\nu_e} < 3.0 \times 10^{-12}\mu_B\,.$$

For the magnetic moment of the muon-neutrino, the current best limit has been obtained in the LSND experiment[18]

$$\mu_{\nu_\mu} < 6.8 \times 10^{-10}\mu_B\,.$$

In the case of the electric dipole moment d_{ν_e}, d_{ν_μ} the best limits are[20]

$$d_{\nu_e,\nu_\mu} < 2 \times 10^{-21}\ (\mathrm{ecm})\,.$$

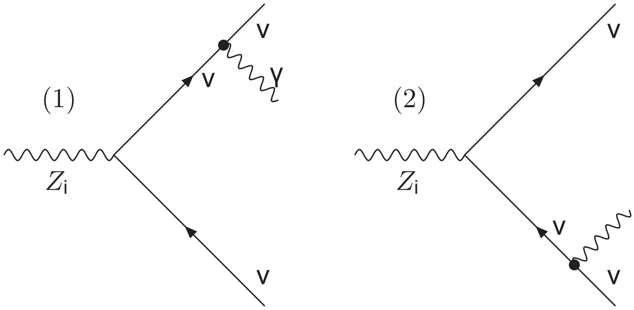

Fig. 2. Feynman diagrams of $Z_i \to \bar{\nu}\nu\gamma$ in the $SU(4)_L \times U(1)_X$ model.

Combining all above conditions leads to the conclusion that the contributions from the ν_e, ν_μ to the cross-section of the process $e^+e^- \to \bar{\nu}\nu\gamma$ are negligible in comparison with ν_τ.

The total cross-section of the process $e^+e^- \to \bar{\nu}_\tau\nu_\tau\gamma$ can be calculated using Breit–Wigner resonance form[67]

$$\sigma(e^+e^- \to \bar{\nu}_\tau\nu_\tau\gamma) = \sum_{i=1}^{3} \frac{4\pi(2J+1)\Gamma_{e^+e^-}\Gamma_{\bar{\nu}_\tau\nu_\tau\gamma}}{\left(s - M_{Z_i}^2\right)^2 + M_{Z_i}^2\Gamma_{Z_i}^2}\,, \tag{16}$$

where Z_i, $i = 1, 2, 3$ are the SM Z boson and two new neutral bosons, respectively, and $\Gamma_{e^+e^-}$, $\Gamma_{\bar{\nu}_\tau\nu_\tau\gamma}$ are the respectively decay width of Z_i in the channel e^+e^- and $\nu\bar{\nu}$, γ (see Fig. 2).

The decay of Z_i to e^+e^- has the same structure as the decay of Z boson in to e^+e^-. The latter is given by[67]

$$\Gamma_{(Z_1 \to e^+e^-)} = \frac{\alpha M_{Z_1}}{12} \frac{\left[g_V^2(e) + g_A^2(e)\right]}{s_W^2(1 - x_2)}\,,$$

where $\alpha = \frac{e^2}{4\pi}$ is the fine structure constant.

The decay rate of Z_i to e^+e^- can be calculated as

$$\Gamma_{(Z_i \to e^+e^-)} = \Gamma_{(Z_1 \to e^+e^-)} \frac{M_{Z_i}}{M_{Z_1}} \frac{\left[g_{iV}^2(e) + g_{iA}^2(e)\right]}{\left[g_{1V}^2(e) + g_{1A}^2(e)\right]}\,.$$

Therefore, we can approximate Γ_{Z_i} as

$$\Gamma_{Z_i} = \frac{M_{Z_i}}{M_{Z_1}}\Gamma_{Z_1}\,.$$

In the following, we will investigate the decay of $Z_i(p)$ into $\bar{\nu}(k_1)\nu(k_2)\gamma(q)$. The Feynman amplitude of the above decay is

$$\begin{aligned}
\mathcal{M}_1(\bar{\nu}\nu\gamma) &= \epsilon^\mu(p)\epsilon^\nu(q)\left[\bar{u}(k_2)\Gamma_\mu \frac{i(\not{k} + m_\nu)}{(k^2 - m_\nu^2)} \frac{(-ig)}{2c_W}\gamma_\nu[g_{iV}(\nu) - g_{iA}(\nu)\gamma_5]v(k_1)\right],\\
\mathcal{M}_2(\bar{\nu}\nu\gamma) &= \epsilon^\mu(p)\epsilon^\nu(q)\left[\bar{u}(k_2)\frac{(-ig)}{2c_W}\gamma_\nu[g_{iV}(\nu) - g_{iA}(\nu)\gamma_5]\frac{i(\not{k} + m_\nu)}{(k^2 - m_\nu^2)}\Gamma_\mu v(k_1)\right],
\end{aligned} \tag{17}$$

where

$$\Gamma^{\alpha} = eF_1(q^2)\gamma^{\alpha} + \frac{ie}{2m_{\nu}}F_2(q^2)\sigma^{\alpha\mu}q_{\mu} + eF_3(q^2)\gamma_5\sigma^{\alpha\mu}q_{\mu}$$

is the tau-neutrino electromagnetic vertex, e is the charge of the electron, q^{μ} is the photon momentum and $F_{1,2,3}(q^2)$ are the electromagnetic form factors of the neutrino, corresponding to charge radius, MM and EDM, respectively, at $q^2 = 0$,[68] while ϵ^{ν} is the polarization vector of the photon and p and k stand for the momenta of the Z and neutrino, respectively. In (17), the polarization of vector fields and helicity of spinor ones are understood.

Summing over spin (s) and averaging out the Z_i polarization (λ), the square of the scattering amplitude is given by

$$\sum_{s,\lambda} |\mathcal{M}_{1,2}|^2 = \frac{g^2}{4\cos^2\theta_W}\left(\mu^2_{\nu_\tau} + d^2_{\nu_\tau}\right) \times \left[\left(g^2_{iV}(\nu) + g^2_{iA}(\nu)\right)\left(s - 2\sqrt{s}E_{\gamma}\right) + g^2_{iA}(\nu)E^2_{\gamma}\sin^2\theta_{\gamma}\right],$$

where θ_{γ} is an angle between momenta of the photon and the neutrino. The decay rate of gauge boson $Z_i \to \nu\bar{\nu}\gamma$ is therefore calculated as

$$\Gamma_{(Z_i\to\nu\bar{\nu}\gamma)} = \int \frac{\alpha\left(\mu^2_{\nu_\tau} + d^2_{\nu_\tau}\right)}{64\pi^2 M_{Z_i} x_W(1 - x_W)}\left[\left(g^2_{iV}(\nu) + g^2_{iA}(\nu)\right)\left(s - 2\sqrt{s}E_{\gamma}\right) + g^2_{iA}(\nu)E^2_{\gamma}\sin^2\theta_{\gamma}\right]E_{\gamma}\,dE_{\gamma}\,d\cos\theta_{\gamma}\,.$$

Substituting the above expression into (16), we have the total cross-section of the process $e^+e^- \to \bar{\nu}_\tau\nu_\tau\gamma$

$$\sigma(e^+e^- \to \nu\bar{\nu}\gamma) = \sum_{i=1,2,3}\int E_{\gamma}\,dE_{\gamma}\,d\cos\theta_{\gamma}\frac{\alpha^2\left(\mu^2_{\nu_\tau} + d^2_{\nu_\tau}\right)}{192\pi}\frac{\left[g^2_{iV}(e) + g^2_{iA}(e)\right]}{x^2_W(1 - x_W)^2} \times \frac{\left[\left(g^2_{iV}(\nu) + g^2_{iA}(\nu)\right)\left(s - 2\sqrt{s}E_{\gamma}\right) + g^2_{iA}(\nu)E^2_{\gamma}\sin^2\theta_{\gamma}\right]}{\left(s - M^2_{Z_i}\right)^2 + M^2_{Z_i}\Gamma^2_{Z_i}}\,. \quad (18)$$

4. Results and Conclusions

The procedure for evaluating discovery significance was reviewed in Refs. 67 and 69. The number of expected single photon events, $N_{\rm exp}$, is assumed to have Gaussian distribution and equals the number of signal (N_S) plus the number of background events (N_B), $N_{\rm exp} = N_S + N_B$. The background is assumed to have Poisson distribution with mean N_B and standard deviation $1\sigma = \sqrt{N_B}$. In Ref. 28 no signal was observed and 6 initial radiation events were found as real background with the angular interval $-0.7 < \cos\theta_{\gamma} < 0.7$. At 68% ($1\sigma$) the number of expected events is then smaller than the upward fluctuation of the background, $N_{\rm exp} \le N_B + \sqrt{N_B}$. This is good approximation only when Poisson distribution approach Gaussian distribution meaning when N_B is large enough ($N_B > 10$). In this work, we roughly approximate with the real background, $N_B = 6$ events. At 1σ, limits on parameters can be found by solving

$$N_{\rm exp} \approx \sigma(\mu_{\nu_\tau}, d_{\nu_\tau})\mathcal{L} \leq 6 + \sqrt{6}\,. \qquad (19)$$

The L3 detector requires energy cluster must be greater than 15 GeV and its polar angle must lie in the range $20° < \theta < 34.5°$, $44.5° < \theta < 135.5°$. Therefore, θ_γ will be integrated over from 44.5° to 135.5° and E_γ from 15 GeV to 100 GeV. The following numerical values are used:[67] $\sin^2\theta_W = 0.23126 \pm 0.00022$, $M_Z = 91.1876 \pm 0.0021$ GeV, $\Gamma_Z = 2.4952 \pm 0.0023$ GeV. We approximate the mass of the two new neutral bosons are of the same order $\left(M_{Z_2} \approx M_{Z_3}\right)$. Hence, the decay rate can be approximated to have the same order $\Gamma_{Z_2} \approx \Gamma_{Z_3}$.

The mass of Z_2, Z_3 bosons can be approximated as $M_{Z_{2,3}} = x_r M_{Z_1}$ where $x_r = \frac{M_{Z_2}}{M_{Z_1}}$ and the decay width of the Z_2, Z_3 bosons are approximated as: $\Gamma_{Z_{2,3}} = x_r \Gamma_{Z_1}$. The mass range of the new neural gauge boson investigated is $\mathcal{O}$ (1.3–3.9) TeV (Refs. 67 and 70) which is equivalent to $x_r \in (15, 40)$. In s-channel, at the Z' resonance, one possibility of the background of the process single photon + "missing energy" is the process $e^+e^- \to \bar{l}l \to \bar{l}l\gamma$ in which the pair of lepton escape the detection. To eliminate this background, the cut requirement is applied with $44.5° < \theta_\gamma < 135.5°$ and $E_\gamma \in [15, 100\text{ GeV}]$.

We obtained the cross-section of the process $e^+e \to \bar{\nu_\tau}\nu_\tau\gamma$: $\sigma = \sigma\big(\mu_{\nu_\tau}, d_{\nu_\tau}, \sqrt{s}, x_r\big)$. We will evaluate the cross-section as a function of the parameters of the model, x_r, which is the ratio of the symmetry breaking scale of the group $SU(4)_L$ and the vacuum expectation value of the $SU(2)_L$ and the center-of-mass energy. Using Eq. (19) for the number of expected events $N_{\rm exp}$ at 1σ, 2σ, 3σ, we can set the bounds of the tau-neutrino magnetic dipole moments with $d_{\nu_\tau} = 0$ for different integrated luminosity $\mathcal{L}$. This analysis can be used to obtain the bound on the tau-neutrino electric dipole moment with $\nu_\tau = 0$.

We will first calculate the magnetic moment for tau-neutrino at center-of-mass energy $\sqrt{s} = 189$ GeV and luminosity $\mathcal{L} = 176\text{ pb}^{-1}$ as at the L3.[29] At 90% we obtain $\mu_{\nu_\tau} < 2.21 \times 10^{-7}$. The limit of magnetic moment is improved by an order of magnitude comparing to the result of the L3[28] experiment.

In the following we will calculate the μ_{ν_τ} magnetic moment and d_{ν_τ} electric dipole moment at the center-of-mass and luminosity at the ILC.[62] We present the bounds obtained on the μ_{ν_τ} magnetic moment and d_{ν_τ} electric dipole moment in Table 2 to demonstrate the order of magnitude. From Table 2 we can see that our result is better than those given in literature[30,45–51,54,55] and in agreement with Refs. 52 and 53.

In the case of the electric dipole moment, our result shows that these bounds are of order 10^{-19} for the 95% C.L. sensitivity limits at 1000 GeV center-of-mass energies and integrated luminosity of 1000 fb^{-1}. These bounds are improved by 2–3 orders of magnitude than those reported in the literature.[45–51,54,55]

In Fig. 3 we evaluate the differential cross-section as a function of photon energy. From Fig. 3, we see that the differential cross-section increases with the energy of

Table 2. Bounds on the μ_{ν_τ} magnetic moment and d_{ν_τ} electric dipole moment for $\sqrt{s} = 0.25, 0.5, 1$ TeV and $\mathcal{L} = 250, 500, 1000$ fb^{-1} at 1σ, 2σ, 3σ.

$\mathcal{L} = 250,\ 500,\ 1000$ fb^{-1}		
$\sqrt{s} = 250$ GeV; $x_r = 15$		
C.L.	$\lvert\mu_{\nu_\tau}(\mu_B)\rvert$	$\lvert d_{\nu_\tau}(\mathrm{e \cdot cm})\rvert$
1σ	$(7.68, 5.43, 3.84) \times 10^{-9}$	$(3.25, 2.3, 1.62) \times 10^{-19}$
2σ	$(8.72, 6.17, 4.36) \times 10^{-9}$	$(3.69, 2.61, 1.84) \times 10^{-19}$
3σ	$(9.65, 6.8, 4.83) \times 10^{-9}$	$(4.1, 2.89, 2.04) \times 10^{-19}$
$\sqrt{s} = 500$ GeV; $x_r = 30$		
C.L.	$\lvert\mu_{\nu_\tau}(\mu_B)\rvert$	$\lvert d_{\nu_\tau}(\mathrm{e \cdot cm})\rvert$
1σ	$(1.71, 1.21, 0.86) \times 10^{-8}$	$(7.26, 5.13, 3.63) \times 10^{-19}$
2σ	$(1.95, 1.38, 0.97) \times 10^{-8}$	$(8.24, 5.82, 4.12) \times 10^{-19}$
3σ	$(2.15, 1.52, 1.1) \times 10^{-8}$	$(9.12, 6.45, 4.56) \times 10^{-19}$
$\sqrt{s} = 1000$ GeV; $x_r = 40$		
C.L.	$\lvert\mu_{\nu_\tau}(\mu_B)\rvert$	$\lvert d_{\nu_\tau}(\mathrm{e \cdot cm})\rvert$
1σ	$(3.51, 2.48, 1.76) \times 10^{-8}$	$(1.49, 1.05, 0.74) \times 10^{-18}$
2σ	$(4.0, 2.82, 2.0) \times 10^{-8}$	$(1.69, 1.19, 0.85) \times 10^{-18}$
3σ	$(4.4, 3.12, 2.2) \times 10^{-8}$	$(1.87, 1.32, 0.94) \times 10^{-18}$

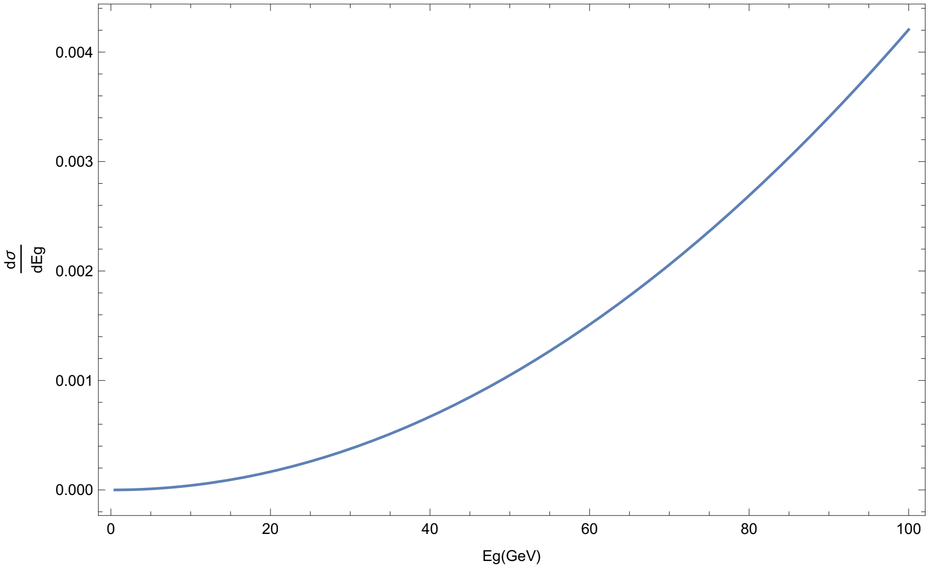

Fig. 3. The differential cross-section for $e^+e^- \to \bar{\nu}\nu\gamma$ as a function of the photon energy Eg.

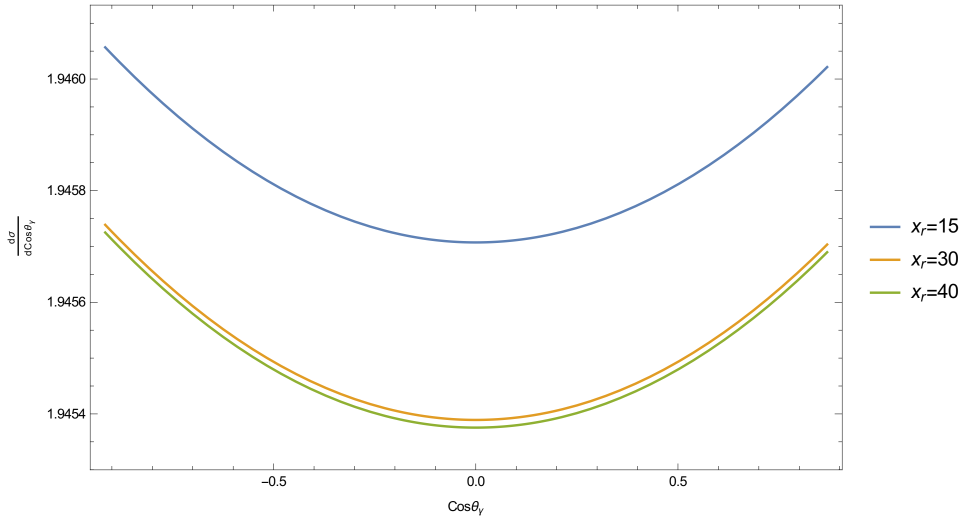

Fig. 4. The differential cross-section for $e^+e^- \to \bar{\nu}\nu\gamma$ as a function of the photon distribution angle $\cos\theta_\gamma$ for different value of Z' mass.

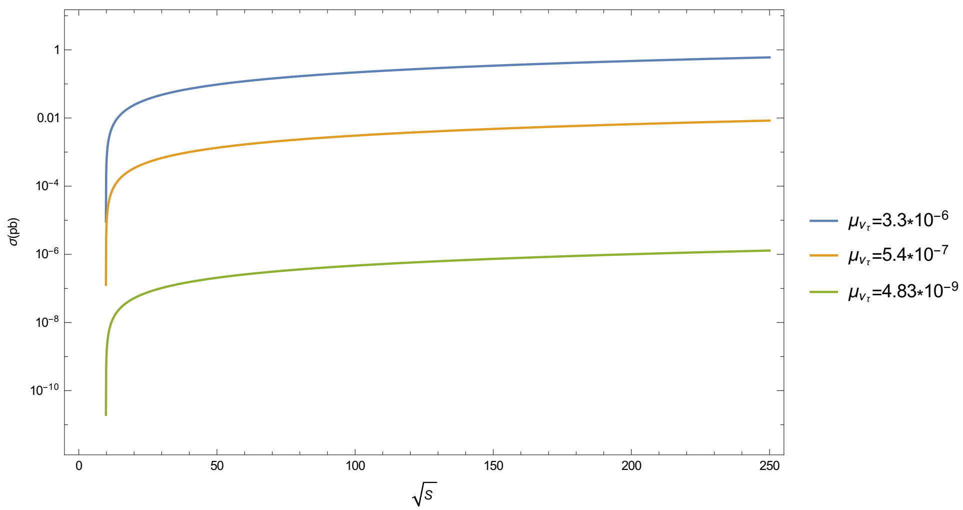

Fig. 5. The cross-section for $e^+e^- \to \bar{\nu}\nu\gamma$ as a function of the center-of-mass energy $\sqrt{s}$ for different value of magnetic moment.

the photon. At energy smaller than 10 GeV the differential cross-section is negligible which is in agreement with the energy cut requirement for photon energy.

In Fig. 4, we evaluate the differential cross-section as a function of the photon distribution angle $\cos\theta_\gamma$ for different value of Z_i mass. The figure shows the symmetrical distribution of the photon in polar angle.

In Fig. 5, we evaluate the cross-section as a function of the center-of-mass energy $\sqrt{s}$ for different value of μ_{ν_τ}. The figure shows the rapid increase starting at

$\sqrt{s} \approx 10$ GeV. The shape of the curves does not change and there is only a shift depending on the values of the magnetic moment.

In summary, we conclude that the estimated limits for the tau-neutrino magnetic and electric dipole moments in the context of an $SU(4)_L \times U(1)_X$ model compare favorably with the limits obtained by the accelerator based experiment such as L3 Collaboration, E827 and CERN-WA-066. Our study complements previous studies on the dipole moments.

It is worth mentioning that recently the Z' boson is well motivated topic connecting with potential discovery of right-handed neutrino (RHN) at the LHC.[61] In Ref. 60, the authors have showed that in the framework of the 3-3-1 model with RHN, the result is positive if masses of the Z' boson and of right-handed neutrinos are around 4 TeV and 200 GeV, respectively. For the above-mentioned result, the decay width of $Z' \to l\bar{l}$ has been evaluated. Return back to our study, the bounds derived here will affect to other channels, especially on the decay $Z' \to l\bar{l}$. We will return to this subject in the future study.

Acknowledgments

This research is funded by the Vietnam National Foundation for Science and Technology Development (NAFOSTED) under Grant No. 103.01-2017.356. H. N. Long acknowledges the financial support of the Vietnam Academy of Science and Technology under Grant No. NVCC05.01/19-19.

References

1. SNO Collab. (Q. R. Ahmad *et al.*), *Phys. Rev. Lett.* **87**, 071301 (2001).
2. SK Collab. (Y. Fukuda *et al.*), *Phys. Rev. Lett.* **81**, 1562 (1998).
3. W. J. Marciano and A. I. Sanda, *Phys. Lett. B* **67**, 303 (1977).
4. B. W. Lee and R. E. Shrock, *Phys. Rev. D* **16**, 1444 (1977).
5. J. Bernstein, M. Ruderman and G. Feinberg, *Phys. Rev.* **132**, 1227 (1963).
6. L. B. Okun, M. B. Voloshin and M. I. Vysotky, *Sov. Phys. JETP* **64**, 446 (1986).
7. O. G. Miranda *et al.*, *Nucl. Phys. B* **595**, 360 (2001).
8. O. G. Miranda *et al.*, *Phys. Lett. B* **521**, 299 (2001).
9. S. L. Glashow, *Nucl. Phys.* **22**, 579 (1961).
10. S. Weinberg, *Phys. Rev. Lett.* **19**, 1264 (1967).
11. A. Salam, *Elementary Particle Theory*, ed. N. Svartholm (Almquist and Wiskell, Stockholm, 1968), p. 367.
12. K. Fujikawa and R. Shrock, *Phys. Rev. Lett.* **45**, 963 (1980).
13. TEXONO Collab. (H. T. Wong *et al.*), *Phys. Rev. D* **75**, 012001 (2007).
14. GEMMA Collab. (A. G. Bed *et al.*), *Adv. High Energy Phys.* **2012**, 350150 (2012).
15. Borexino Collab. (C. Arpesella *et al.*), *Phys. Rev. Lett.* **101**, 091302 (2008).
16. DONUT Collab. (R. Schwinhorst *et al.*), *Phys. Lett. B* **513**, 23 (2001).
17. WA66 Collab. (A. M. Cooper-Sarkar *et al.*), *Phys. Lett. B* **280**, 153 (1992).
18. LSND Collab. (L. B. Auerbach *et al.*), *Phys. Rev. D* **63**, 112001 (2001).
19. G. G. Raffelt, *Phys. Rep.* **320**, 319 (1999).
20. F. del Aguila and M. Sher, *Phys. Lett. B* **252**, 116 (1990).

21. D. Fargion, M. Yu. Khlopov, R. V. Konoplich and R. Mignani, *Phys. Rev. D* **54**, 4684 (1996).
22. S. Y. Choi, J. S. Shim, H. S. Song, J. Song and C. Yu, *Phys. Rev. D* **60**, 013007 (1999).
23. J. L. Lopez, D. V. Nanopoulos and A. Zichichi, *Phys. Rev. D* **55**, 5813 (1997).
24. M. Fukugita and T. Yanagida, *Physics of Neutrinos and Applications to Astrophysics* (Springer, Berlin, 2003).
25. A. Cisneros, *Astrophys. Space Sci.* **10**, 87 (1971).
26. R. Escribano and E. Massó, *Phys. Lett. B* **395**, 369 (1997).
27. K. Akama, T. Hattori and K. Katsuura, *Phys. Rev. Lett.* **88**, 201601 (2002).
28. L3 Collab. (M. Acciarri *et al.*), *Phys. Lett. B* **412**, 201 (1997).
29. L3 Collab., *Phys. Lett. B* **470**, 268 (1999).
30. T. M. Gould and I. Z. Rothstein, *Phys. Lett. B* **333**, 545 (1994).
31. M. Sher and S. Nie, *Phys. Rev. D* **65**, 093018 (2002).
32. G. Senjanovic, *Nucl. Phys. B* **153**, 334 (1979).
33. G. Senjanovic and R. N. Mohapatra, *Phys. Rev. D* **12**, 1502 (1975).
34. U. Baur *et al.*, *Phys. Rev. D* **35**, 297 (1987).
35. F. Pisano and V. Pleitez, *Phys. Rev. D* **46**, 410 (1992).
36. P. H. Frampton, *Phys. Rev. Lett.* **69**, 2889 (1992).
37. R. Foot, O. F. Hernandez, F. Pisano and V. Pleitez, *Phys. Rev. D* **47**, 4158 (1993).
38. R. Foot, H. N. Long and T. A. Tran, *Phys. Rev. D* **50**, 34 (1994).
39. M. Singer, J. W. F. Valle and J. Schechter, *Phys. Rev. D* **22**, 738 (1980).
40. J. C. Montero, F. Pisano and V. Pleitez, *Phys. Rev. D* **47**, 2918 (1993).
41. H. N. Long, *Phys. Rev. D* **54**, 4691 (1996).
42. W. A. Ponce, Y. Giraldo and L. A. Sanchez, *Phys. Rev. D* **67**, 075001 (2003).
43. P. V. Dong, H. N. Long, D. T. Nhung and D. V. Soa, *Phys. Rev. D* **73**, 035004 (2006).
44. P. V. Dong and H. N. Long, *Adv. High Energy Phys.* **2008**, 739492 (2008).
45. A. Gutiérrez-Rodríguez *et al.*, *Eur. Phys. J. C* **71**, 1819 (2011).
46. A. Gutiérrez-Rodríguez *et al.*, *Pramana* **79**, 903 (2012).
47. M. A. Hernández-Ruíz, A. Gutiérrez-Rodríguez, C. P. Castañeda-Almanza, A. Espinoza-Garrido and A. Chubykalo, *Nucl. Phys. B* (*Proc. Suppl.*) **253-255**, 204 (2014).
48. A. Gutiérrez-Rodríguez, *Int. J. Theor. Phys.* **54**, 236 (2015).
49. A. Gutiérrez-Rodríguez, M. A. Hernández-Ruíz, A. Rosado and M. Maya, *Rev. Mex. Fis.* **45**, 249 (1999).
50. A. Gutiérrez-Rodríguez and M. A. Hernández-Ruíz, *Acta Phys. Slov.* **53**, 293 (2003).
51. A. Gutiérrez-Rodríguez, *Adv. High Energy Phys.* **2014**, 491252 (2014).
52. A. Llamas-Bugarin, A. Gutiérrez-Rodríguez and M. A. Hernández-Ruíz, *Phys. Rev. D* **95**, 116008 (2017).
53. A. Gutiérrez-Rodríguez, M. Koksal, A. A. Billur, M. A. Hernández-Ruíz, arXiv:1712.02439 [hep-ph].
54. A. Gutiérrez-Rodríguez, M. A. Hernández-Ruíz, B. Jayme-Valdés and M. A. Pérez, *Phys. Rev. D* **74**, 053002 (2006).
55. A. Aydemir and R. Sever, *Mod. Phys. Lett. A* **16**, 457 (2001).
56. F. Pisano and V. Pleitez, *Phys. Rev. D* **51**, 3865 (1995).
57. A. Palcu, *Phys. Rev. D* **85**, 113010 (2012).
58. H. N. Long, L. T. Hue and D. V. Loi, *Phys. Rev. D* **94**, 015007 (2016).
59. M. B. Voloshin, *Sov. J. Nucl. Phys.* **48**, 512 (1988).
60. F. F. Freitas, C. A. de S. Pires and P. Vasconcelos, *Phys. Rev. D* **98**, 035005 (2018).

61. P. Cox, C. Han and T. T. Yanagida, *J. High Energy Phys.* **01**, 037 (2018).
62. T. Abe *et al.*, Linear collider physics resource book for Snowmass 2001 — Part 3: Studies of exotic and standard model physics, http://arxiv.org/abs/hep-ex/0106057.
63. E. Accomando *et al.*, Physics at the CLIC multi-TeV linear collider, http://arxiv.org/abs/hep-ph/0412251v1.
64. S. Y. Choi *et al.*, *Phys. Rev. D* **60**, 013007 (1999).
65. D. Bardin *et al.*, *Eur. Phys. J. C* **24**, 373 (2002).
66. X. Qian and P. Vogel, *Prog. Part. Nucl. Phys.* **83**, 1 (2015).
67. Particle Data Group (C. Patrignani *et al.*), *Chin. Phys. C* **40**, 100001 (2016).
68. R. Escribano and E. Massó, *Phys. Lett. B* **395**, 369 (1997).
69. R. S. Gupta and J. D. Wells, *Phys. Lett. B* **710**, 154 (2012).
70. CMS Collab. (S. Chatrchyan *et al.*), *Phys. Rev. D* **87**, 072002 (2013).